

# Mechanism of reinforcement from two field trials

R.Arab, P.Villard & J.P.Gourc  
IRIGM-Lgm, Grenoble University, France

**ABSTRACT :** The finite element method is used to simulate the behaviour of two field trials reinforced soil wall models, one reinforced with non woven geotextile, the other with woven geotextile. The experimental results shown the specific behaviour of this kind of structure : Until 2/3 of failure load, the displacements occurred were very small. To explain these specific characteristics, simulations were carried out, taking into consideration the state of great strains below the loading slab and the compacting effect.

## 1 INTRODUCTION

Geosynthetic-reinforced soil retaining wall are gaining a wide acceptance for replacing conventional retaining walls because of cost-effectiveness and proved performance.

In France, the association of geosynthetic-reinforced soil with cellular facing has been widely used for making steeper highway embankment slope (Gourc et al. 1990). To extend their application to bridge abutment and to understand the behaviour of this kind of structures in these conditions, two full scale experimentations on walls loaded on top were conducted as part of the GARDEN project (Gourc and al, 1995) in collaboration with French Ministry, Scetauroute Society and I.R.I.G.M - L.g.m. The two walls were backfilled with sand, one reinforced by non woven geotextile and one other by woven geotextile.

Geosynthetic-reinforced soil represents one of the most sophisticated soil-structure interaction problems. The FE procedure is a useful tool for this structure type, and was used by many authors, (Smith and al, 1992), (Gourc and al, 1992).

In this study, the computer program (GOLIATH) developed at the I.R.I.G.M-L.g.m was used.

In order to simulate the physical phenomenon observed, some assumptions were done : two displacement approaches were used and a tentative of introduction of the compacting effect was carried out by applying a uniform surcharge on the top of the wall.

## 2 MEASUREMENT RESULTS

The instrumented walls (Fig. 1), basic reference of the numerical modelling were 4.35 m high by 5 m wide.

The reinforcement distribution in the two profiles reinforced embankment are not exactly the same, this is justified by the difference in mechanical properties between the two geotextiles.

The soil used to construct the embankment was a fine sand excavated from the site. The soil was placed and compacted to a bulk unit weight of 19 kN/m<sup>3</sup> which correspond to the standard Proctor density (14.2 %).

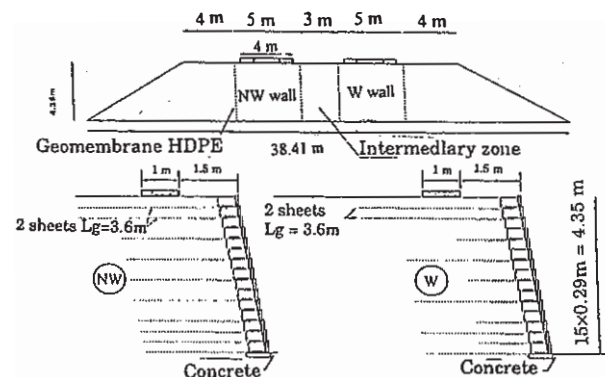


Fig. 1 Front view and profile of the reinforcement embankment

Results from triaxial compression tests indicated that the soil exhibits a friction angle  $\phi = 36-42^\circ$  and a cohesion  $c = 4$  kPa.

The reinforcement used were a non woven (NW) geotextile reinforcement for the profile at the left side on figure 1 and a woven (W) geotextile reinforcement knitted to a non-woven sheet for the profile at the right side. The failure characteristics are :  $T_f = 25$  kN/m,  $\epsilon_f = 30\%$  for NW geotextile and  $T_f = 44$  kN/m,  $\epsilon_f = 15\%$  for NW geotextile. The tensile tests of the two geotextiles in the working direction are illustrated in figure 2.

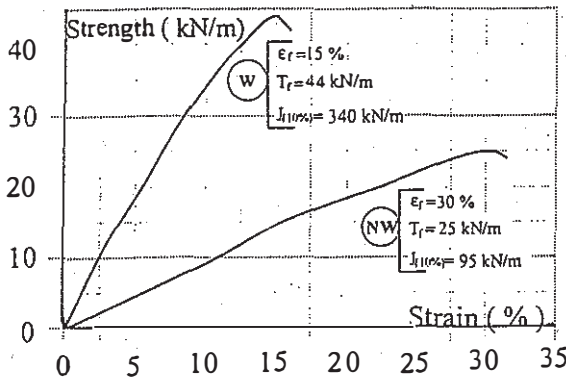


Fig. 2 Tensile tests on the two geotextiles

The main results measured for the two walls are slab load settlement (Fig. 3), wall face deflection (Fig. 4 and 5) and the strain distribution in the instrumented sheets (Fig. 6 and 7).

In both cases the experimental results (Fig. 3) show an interesting point of this kind of structures, until 2/3 of failure load, only small displacements were occurred below the slab load. The load-settlement curves presents two straight lines, each one with a different slope.

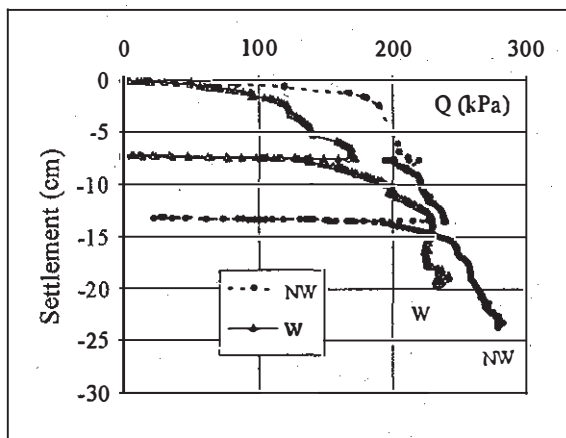


Fig. 3 Concrete slab load settlement versus surcharge

As we can see it in figures 4 and 5, the woven wall (W) fails by overturning and the non-woven one by bulging.

The strain distribution in the instrumented sheets (Fig. 6 and 7) are similar for the two structures, although the failure mechanisms are not the same.

The measured settlement of the structure foundation were very small.

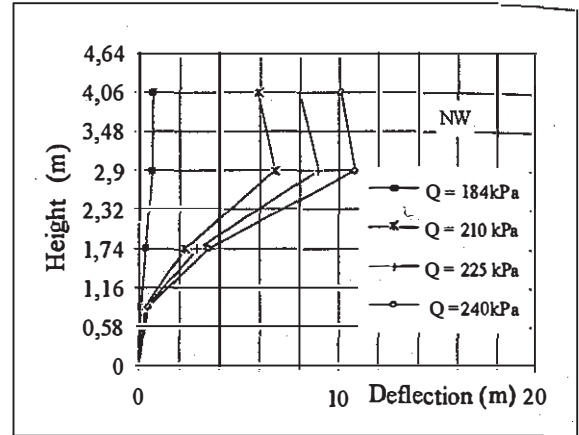


Fig. 4 Wall face deflection (NW wall)

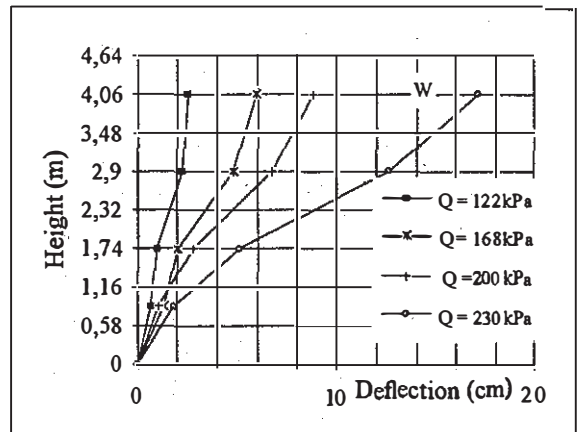


Fig. 5 Wall face deflection (W wall)

For the two profiles, at failure, cracks were occurred, first at the back of the slab load after that, at the rear extremity of the upper sheet.

The cracks behind the concrete slab were induced by punching and the ones observed at the rear extremity of the upper sheet by slippage.

As the space between the geotextile sheets was very short, the soil between was highly confined and stiffened forming a composite material that behaves as a monolithic block.

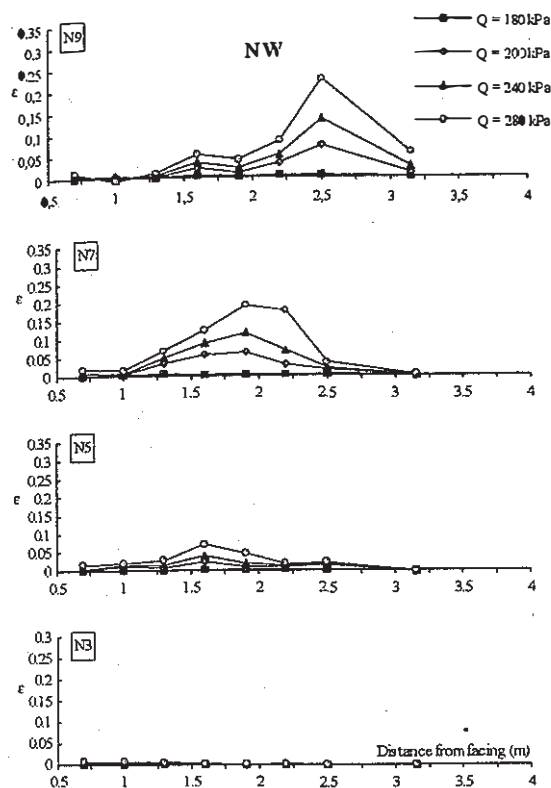


Fig. 6 Strain distribution measured in the reinforcement (NW wall)

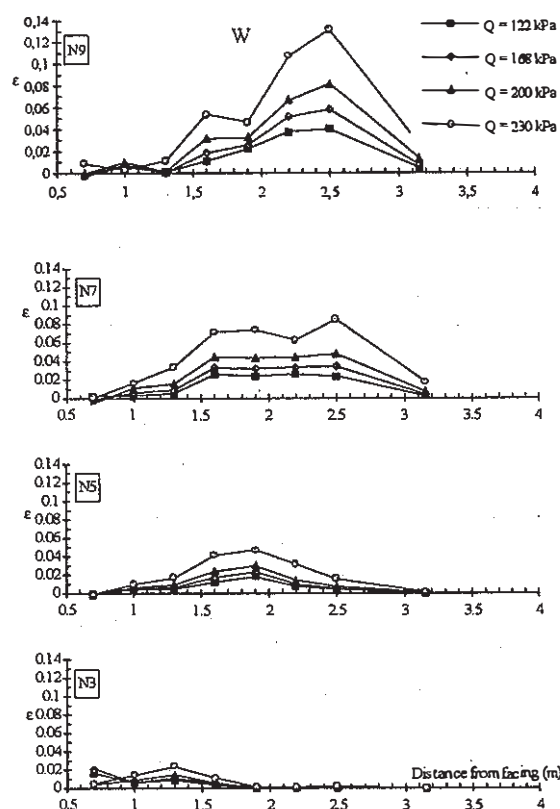


Fig. 7 Strain distribution measured in the reinforcement (W wall)

### 3 NUMERICAL MODELLING

A plane strain finite element analysis was used. Figure 8 show the finite element mesh used for the two models. It is composed of 526 nodes, 884 triangular elements, 35 four nodes elements, 140 bar elements for NW wall and 108 bar elements for W wall.

The soil is modelled by three node isoparametric elements. The fill was assumed to be an elastic-perfectly plastic material with a Mohr-Coulomb failure criterion ( $E=20$  MPa,  $\nu=0.3$ ,  $c=4$  kPa,  $\phi=36^\circ$ ) and a unit weight  $\gamma=19$  kN/m<sup>3</sup>. The fill was assumed to have a non associated flow rule with a dilatancy angle  $\psi=6^\circ$ .

The foundation of the wall is supposed to have an elastic behaviour ( $E=60$  MPa,  $\nu=0.33$ ).

The facing is modelled using four node isoparametric elements and was supposed to be elastic ( $E=25$  MPa,  $\nu=0.2$  and a unit weight  $\gamma=22$  kN/m<sup>3</sup>).

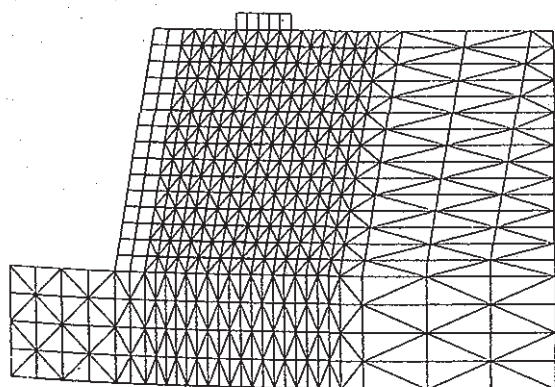


Fig. 8 finite element mesh used

The geotextile sheets were modelled using linear elastic bar elements with negligible compressive strength and no bending stiffness (which allowed the simulation of the membrane behaviour).

The reinforcement stiffness was respectively  $E = 38 \text{ MPa}$  and  $98 \text{ MPa}$  for a non woven and woven geotextile and the thickness of  $3 \text{ mm}$ .

The full height of the wall is initially constructed, applying body forces on the structure with ten load increments of  $0.1g$  then the concentrated load is applied to a linear elastic slab ( $E = 1500 \text{ MPa}$ ,  $\nu = 0.2$ ) with  $10 \text{ kPa}$  increments until  $110 \text{ kPa}$ , followed by  $2.5 \text{ kPa}$  increments until failure. The facing is assumed to be continuous and the sheets are assumed to be fully bonded to the soil (no relative displacement).

### 3.1 Effect of the displacement approaches

Two displacement approaches were used to simulate the two walls :

small displacement approach :

$$\epsilon_{ij} = \frac{1}{2} \left( \frac{\partial u_i}{\partial x_j} + \frac{\partial u_j}{\partial x_i} \right)$$

large displacement approach :

$$\epsilon_{ij} = \frac{1}{2} \left( \frac{\partial u_i}{\partial x_j} + \frac{\partial u_j}{\partial x_i} + \frac{\partial u_k}{\partial x_i} \frac{\partial u_k}{\partial x_j} \right)$$

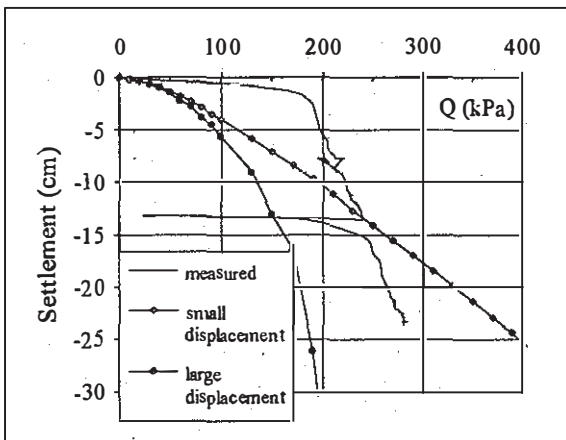


Fig. 9 Slab load settlement versus surcharge predicted and measured results (NW wall)

### Slab settlement :

Figures 9 to 12 illustrate the predicted and the measured slab load settlements and horizontal displacement wall face of the two walls.

From figures 9 and 10, we notice that the displacements calculated for small pressure, in all the simulations carried out are greater than those measured.

The "large displacement" option allow a better approach of the physical phenomenon observed close to the failure.

If results obtained by the large displacement option are satisfactory for the W wall, we are not able to explain in the case of the NW wall the great difference of the failure load predicted.

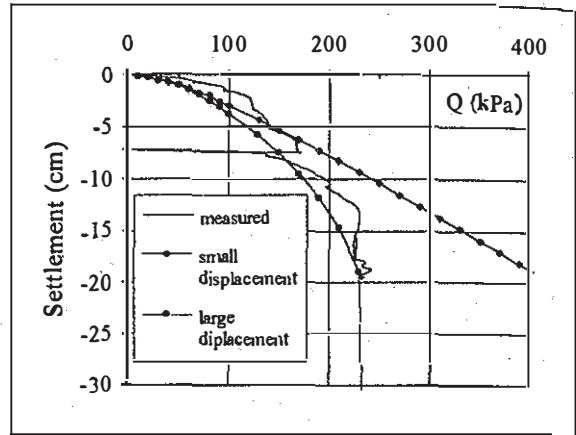


Fig. 10 Slab load settlement versus surcharge predicted and measured results (W wall)

### Wall face deflection :

On figures 11 and 12, we remark that the large displacement approach is more realistic, although the simulation predict a failure by bulging.

The strain distribution calculated with the "large displacement" option are shown in figures 13 and 14. The comparison between the calculated and measured results (Fig. 6, 7, 13 and 14) gives the same conclusions : the difference between the results for W and NW is the punching effect below the slab load stronger in the case of the NW wall.

The line of the maximum tensile force in geotextiles is plotted in figure 15 versus  $x$ , distance from wall face, and  $z$ , depth from the toe of the wall and  $H$  the height. We notice that a reinforcement length required is more than  $0.6 H$ . The option of calculation ("small" and "large displacement") do not influence the location of the maximum tensile load.

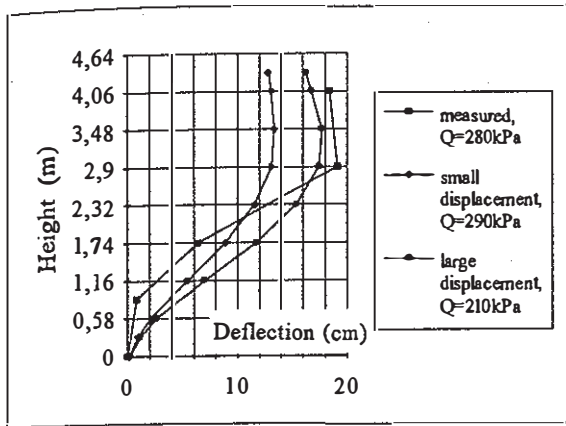


Fig. 11 Wall face deflection (NW wall)

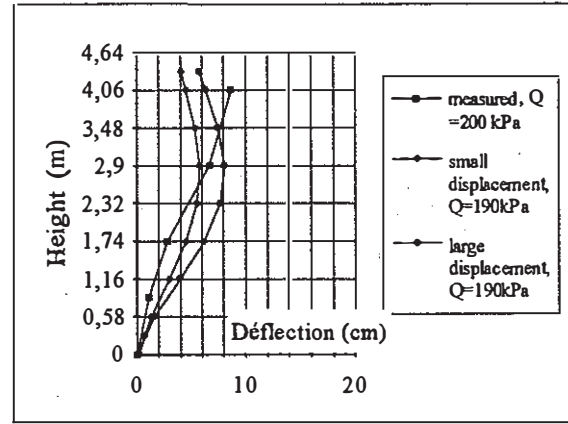


Fig. 12 Wall face deflection (W wall)

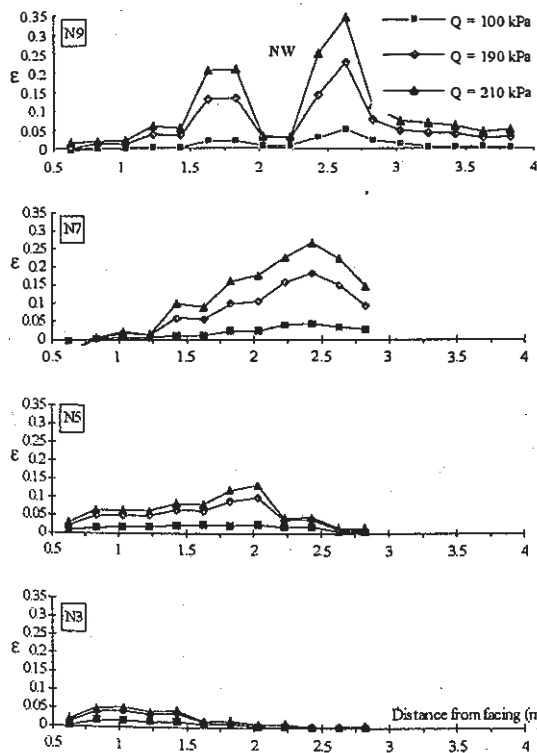


Fig. 13 Strain distribution in the reinforcement, NW wall (large displacement approach)

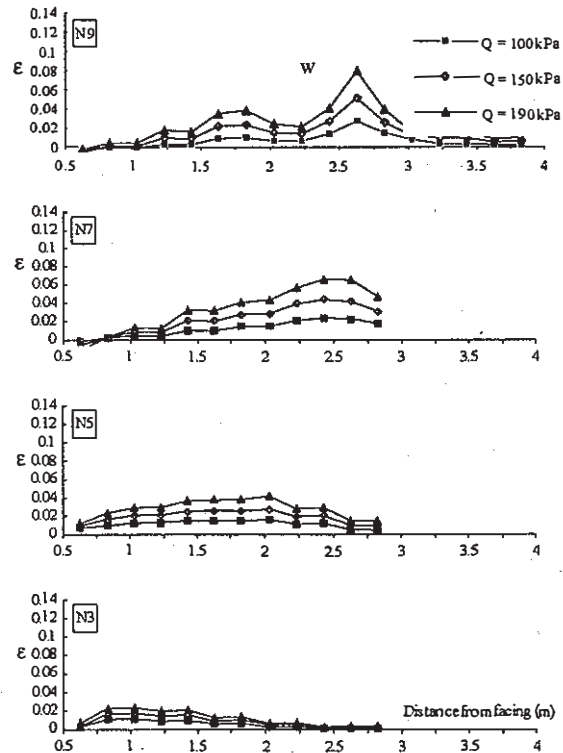


Fig. 14 Strain distribution in the reinforcement, W wall (large displacement approach)

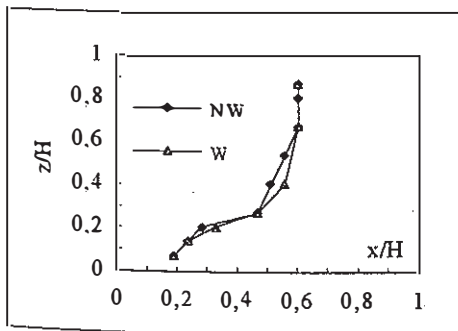


Fig. 15 Maximum tensile loads line

### 3.2 Effect of the compaction

The results obtained from the first calculation for the NW wall don't allow to predict the failure load correctly. One potential reason could be the rough simulation of the construction of the multi - layers structure proposed. In this second step, we propose to simulate the compaction of every soil layer. we attempt to simulate the compacting effect by loading and unloading of an uniform surcharge at the top of the wall (0, 50 and 100 kPa).



These values are justified by the vertical pressure measured below the same compactor in an equivalent embankment about 5 m high (Fig. 16).

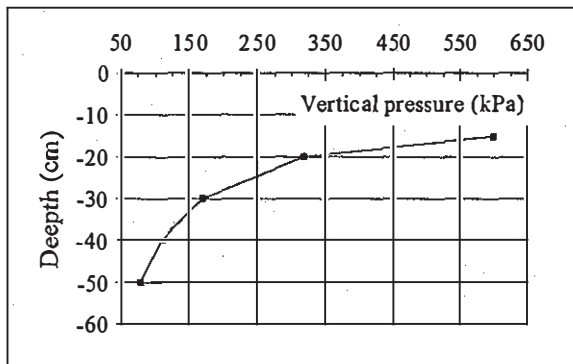


Fig. 16 vertical pressure in an equivalent embankment below the compactor

The settlement of the loading slab plotted in figure 17 represents the settlement induced (after compaction).

The compacting effect induces an increase of the failure load and increase the global stiffness of the structure under small load.

However the modelisation of the compacting effect requires additional experimental and numerical studies for validation.

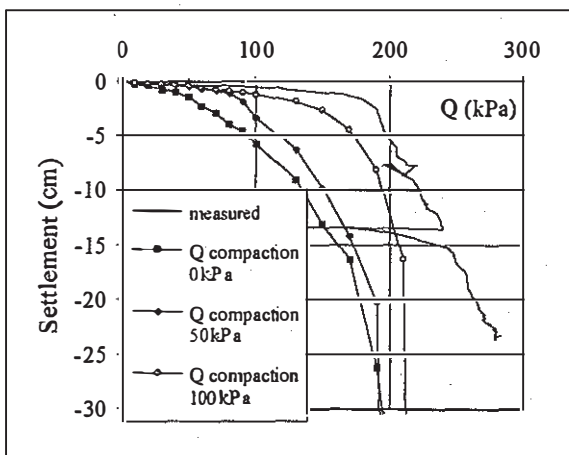


Fig. 17 Slab load settlement versus the localised load (modelisation of the compaction effect)

### 3.3 Parametric study

A parametric study was carried out to investigate the effect of the short sheets for the W wall and the influence of the facing stiffness for the NW wall.

We found that the facing stiffness limits the lateral displacement of the wall. For small top load, the slab

settlement calculated are the same in the two calculations carried out with the two facing stiffness considered ( $E = 5$  and  $25$  MPa).

The calculations carried out shown that the inclusion of woven short sheets have no influence on the global behaviour ; perhaps the short sheets contribute to locally increase the bending stiffness of the facing but the effect is not significative.

## 4 CONCLUSIONS

A finite element method has been used to model two field trials soil walls reinforced with non woven and woven geotextile.

The calculations carried out on the two walls shown that it is important to take into account the compacting effect in order to explain why, until 2/3 of failure load, the displacement occurred were small.

The strong punching effect below the slab load proves the necessity to take into consideration the membrane behaviour of the geotextiles.

A realistic modelisation could be considered by simulating the construction sequences of the structure, however, lack of experimental data on the compaction effect make such approach very difficult.

## REFERENCES

- Duncan J. M. (1994). The role of advanced constitutive relations in practical applications, *State-of-the-art 13th Int. Conf. on soil Mech. and found. Engrg*; pp. 31-48.
- Gourc J.P., Gotteland P.H., Hasa E., Perrier H., Baraize E. (1995) Geotextile reinforced structures as bridge abutments : full scale experimentation, *Geosynthetics 95, Nashville, USA*, pp. 79-93.
- Gourc J.P., Gotteland P., Wilson Jones H. (1990) Cellular retaining wall reinforced by geosynthetics Behaviour and design, *Int. reinf. soil. conf*, Glasgow, Scotland, pp. 41-47.
- Gourc, J.P., Villard, P and Matichard, Y. (1992) Pull-out behaviour of reinforcements Centrifuge tests and theoretical validations, *International Symposium on Earth Reinforcement Practice, Kyushu, Japan*, pp. 425-430.
- Smith. I.M. and Segrestin. P. (1992) Inextensible reinforcements versus extensible ties - FEM comparative analysis of reinforced or stablized earth sructures, *International Symposium on Earth Reinforcement Practice, Kyushu, Japan*, pp. 425-430.